A Simple Model of the Formation and Maintenance of the Shelf/Slope Front in the Middle Atlantic Bight*

DAVID C. CHAPMAN

Woods Hole Oceanographic Institution, Woods Hole, MA 02543

(Manuscript received 4 December 1985, in final form 29 January 1986)

ABSTRACT

The strong salinity and temperature gradients across the shelf/slope front in the Middle Atlantic Bight often compensate such that the cross-front density gradient is nearly eliminated. This suggests that the density field may not be as dynamically important as has been assumed in previous models. Hypothesizing this to be the case, a simple steady barotropic model, which allows no density variations, is used to demonstrate that a strong tracer gradient may form near the shelf break. The velocity field is such that an initially smooth tracer distribution develops a sharp front within a relatively short downstream distance. Essential features of the model are 1) the velocity convergence near the shelf break which acts to sharpen the front on the shelf side, and 2) the increase in bottom slope and depth seaward of the shelf break which leads to rapid diffusion of tracer into the deep ocean. The result is that the front is maintained for a large alongshelf distance despite both diffusion effects and the frictional decay of the alongshelf velocity.

1. Introduction

The shelf/slope front in the Middle Atlantic Bight extends for about 1000 km along the shelf break from Nova Scotia to Cape Hatteras and separates the colder, fresher shelf water from the warmer, saltier slope water (e.g., Wright, 1983; Lyne and Csanady, 1984). The mechanisms by which the shelf/slope front is formed and maintained as well as the factors that determine its location have not been firmly established. For example, Garrett and Horne (1978) concluded that cabbeling and double diffusion are probably not capable of maintaining the front. Further, several two-dimensional (cross-front) models of density fronts (e.g., Wang, 1984; Csanady, 1984; Ou, 1983; Hsueh and Cushman-Roisin, 1983) postulate the existence of the front and then predict velocity fields that are *consistent* with the density front. They do not explain how the front forms nor do they predict how its structure is maintained in the alongshelf direction.

An interesting feature of the shelf/slope front in the Middle Atlantic Bight is that the substantial temperature and salinity gradients across the front often compensate (especially in summer) such that the density contrast is greatly reduced (e.g., Fig. 1; see also Lyne and Csanady, 1984). This suggests that the density field may not be as important in the frontal formation and maintenance processes as has been assumed in most models. In other words, temperature and salinity may behave like passive tracers, and the dynamics of the shelf/slope front in the Middle Atlantic Bight may be largely independent of the detailed density structure near the front. Hypothesizing this to be the case, a simple steady barotropic coastal model, which allows no density variations, is used to demonstrate that a tracer front may form at the shelf break and may be maintained in the alongshelf direction despite both diffusion effects and the frictional decay of the alongshelf velocity. The model is presented in section 2. The results appear in section 3 followed by some discussion of the dynamics in section 4 and a general discussion in section 5.

2. Steady barotropic coastal model

The steady, linearized, vertically averaged equations of motion are

$$-fv = -g\zeta_x - \frac{ru}{h} \tag{1a}$$

$$fu = -g\zeta_y - \frac{rv}{h} \tag{1b}$$

$$(uh)_x + (vh)_y = 0 \tag{1c}$$

in which (x, y) are the offshore and alongshelf directions (with the coast at $x = 0$), (u, v) the (x, y) velocities, ζ the sea surface elevation, f the Coriolis parameter, $r(x)$ the bottom friction coefficient, $h(x)$ the bottom depth, and g the gravitational acceleration. Subscripts denote partial differentiation. From (1c), a transport streamfunction may be defined by

$$uh = \psi_y, \quad vh = -\psi_x. \tag{2}$$

* Woods Hole Oceanographic Institution Contribution No. 6080.

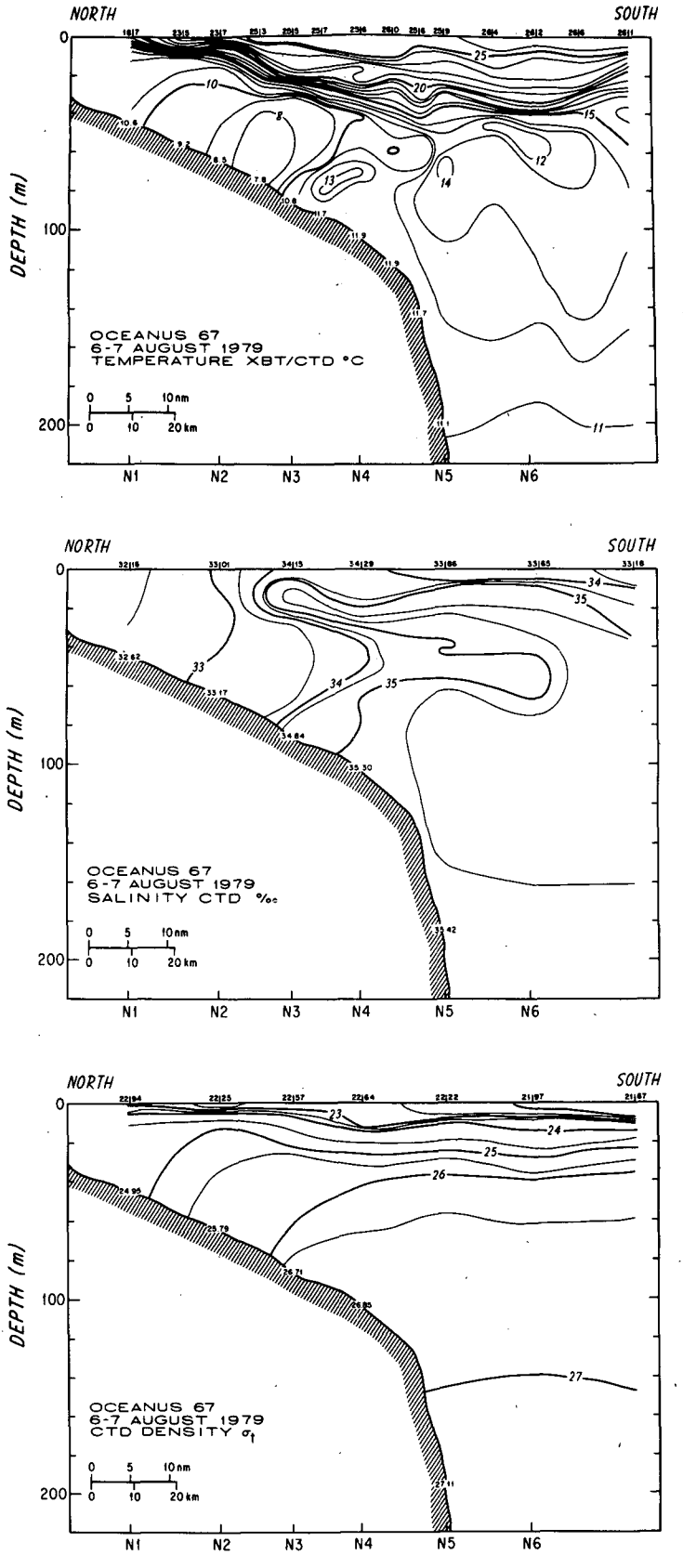

FIG. 1. Temperature, salinity and σ_t sections obtained along the Nantucket Shoals Flux Experiment mooring transect, south of Nantucket Island, on 6–7 August 1979. From Wright (1983).

Using (2), the sea surface elevation can be eliminated from (1a,b) to obtain

$$\psi_{xx} + \psi_{yy} + \frac{fh_x}{r}\psi_y + \left(\frac{r_x}{r} - \frac{2h_x}{h}\right)\psi_x = 0 \qquad (3)$$

where r and h are functions of x only.

The boundary condition of no flow through the coast is satisfied by making the coast a streamline, $\psi = \psi_c$ at $x = 0$. For simplicity, the offshore boundary is a solid wall located well seaward of the shelf break. Without loss of generality, the streamfunction is chosen to be zero at the offshore boundary, $\psi = 0$ at $x = L$. An inflow velocity field is prescribed at the upstream boundary ($y = 0$), while a smoothness condition, $\psi_{yy} = 0$, is applied at the downstream boundary. Solutions of (3), subject to the boundary conditions stated above, have been obtained numerically using the method of Fiadeiro and Veronis (1977).

After obtaining the streamfunction field, a passive tracer may be introduced at the upstream boundary ($y = 0$) and allowed to advect and diffuse through the velocity field. The distribution of depth-averaged tracer ϵ is described by

$$(uh\epsilon)_x + (vh\epsilon)_y = (Kh\epsilon_x)_x + (Kh\epsilon_y)_y \qquad (4)$$

where K is the horizontal eddy diffusivity. By using (1c) and (2) and by assuming a constant K, (4) may be simplified to

$$\frac{1}{h}(\psi_y\epsilon_x - \psi_x\epsilon_y) = K\left(\epsilon_{xx} + \frac{h_x}{h}\epsilon_x + \epsilon_{yy}\right). \qquad (5)$$

This is a standard advection–diffusion equation except for the term involving h_x which represents the apparent increase in diffusion with increasing depth. Physically, as the tracer is spread over a deeper water depth, the depth-averaged concentration must decrease to conserve tracer. Note that this term will be largest where the bottom slope is large in relatively shallow water, i.e., typically just seaward of the shelf break.

The flux of tracer at the coast is assumed zero, $\epsilon_x = 0$ at $x = 0$. Beyond the offshore wall, the deep sea is assumed to contain a uniform tracer distribution which remains unaltered by mixing with the vastly smaller volume of shelf water. The linearity of the model then allows the choice of $\epsilon = 0$ at $x = L$ without loss of generality. The tracer distribution is prescribed at the upstream boundary, while a smoothness condition, $\epsilon_{yy} = 0$, is used at the downstream boundary. Solutions of (5), subject to the boundary conditions stated above, have been obtained numerically by again using the method of Fiadeiro and Veronis (1977).

3. Formation of a shelf/slope front

A simple example using the model described in section 2 illustrates the formation and maintenance of the tracer front. It should be emphasized that the model serves primarily to demonstrate the qualitative features of the proposed mechanism, hence the detailed parameter values used in the calculation are not crucial.

The topography is chosen as a crude representation of the Middle Atlantic Bight. A shelf with bottom slope 10^{-3} adjoins a continental slope with a bottom slope of 0.05 which borders a flat-bottom deep ocean of depth 3110 m;

$$h(x) = \begin{cases} 10 + 0.001x, & 0 < x < 10^5 \text{ m} \\ 110 + 0.05(x - 10^5), & 10^5 < x < 1.6 \times 10^5 \text{ m} \\ 3110, & 1.6 \times 10^5 \text{ m} < x. \end{cases} \qquad (6)$$

The bottom friction is assumed to increase in shallow water. The functional form used by Chapman et al. (1986), which is based roughly on realistic estimates, is assumed here; $r = 0.03 \text{ m}^2 \text{ s}^{-1}/(20 \text{ m} + h) + 0.00015 \text{ m s}^{-1}$. The Coriolis parameter is assumed to be $f = 10^{-4} \text{ s}^{-1}$. The horizontal eddy diffusivity is assumed to be $K = 100 \text{ m}^2 \text{ s}^{-1}$ based on estimates of Davis (1985). Note that this value is an order of magnitude larger than the value assumed by Garrett and Horne (1978) and will be discussed further in section 4.

The mean flow in the Middle Atlantic Bight is apparently a downstream continuation of the mean flow along the Scotian Shelf and along the southern flank of Georges Bank (Chapman et al., 1986). Therefore, the upstream velocity for the model is chosen to represent qualitatively the observed mean flow into the Middle Atlantic Bight from the Scotian Shelf. A uniform inflow ($v = -0.1 \text{ m s}^{-1}$) is imposed within 80 km of the coast and set to zero from there to the offshore wall at $x = L = 240$ km. The resulting total transport is $\psi_T = -0.4 \times 10^6 \text{ m}^3 \text{ s}^{-1}$ which is comparable to the estimated observed transport in the Middle Atlantic Bight (Beardsley et al., 1985). The transport streamfunction, computed on a 25×80 grid with $\Delta x = \Delta y = 10$ km, is contoured in Fig. 2. The streamfunction has been scaled by the total transport ψ_T, so the coastal streamline value is $\psi_c = 1$, and 10 percent of the inflow transport occurs between any two streamlines. As expected the inflow moves toward the shelf break due to bottom friction effects (e.g., Wang, 1982; Chapman et al., 1986). Physically, bottom friction allows the inflow to cross isobaths and to spread throughout the model domain (i.e., with no bottom friction, all flow must be along isobaths). Friction effects decrease with increasing depth so that the flow becomes more nearly along isobaths. Thus, the sharp increase in depth seaward of the shelf break drastically reduces the friction effects and leads to a convergence there. This is seen more clearly in Fig. 3 which shows velocity profiles at several alongshelf locations. The maxima of both alongshelf and cross-shelf velocities occur closer to the shelf break with increasing downstream distance. The maxima also de-

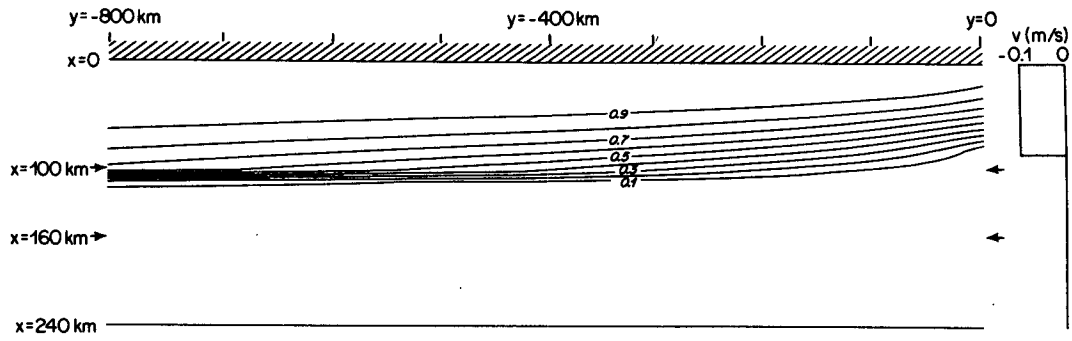

FIG. 2. Plan view of transport streamlines for the model described in section 3. Contour interval is 0.1 × total inflow transport. Inflow velocity profile is shown on the right. The arrows denote the shelf break and the base of the continental slope.

crease in value with downstream distance due to frictional decay and net offshelf transport.

The passive tracer is introduced into this velocity field at the upstream boundary. In order to demonstrate that the velocity field will form a tracer front, the upstream distribution should be smooth and without a front. Here, the distribution $\epsilon_0 = \cos(\pi x/2L)$ at $y = 0$ is chosen because the results can be compared to an analytical solution for a simpler case (section 4). However, virtually any upstream distribution which satisfies the boundary conditions at $x = 0, L$ will evolve into a very similar pattern within ~100 km of the upstream boundary. The resulting tracer distribution is contoured in Fig. 4. Within 50 km of the upstream boundary, the smooth inflow distribution is changed by the flow into a pattern with a strong gradient near the shelf break. This gradient is fairly well maintained for several hundred kilometers although it weakens somewhat in the downstream direction because of both the gradual net loss of tracer to the deep ocean and the weakening of the velocity field. Figure 5 shows the cross-shelf structure of the tracer distribution and of the tracer gradient at several alongshelf locations. Note that the absolute value of the tracer concentration is meaningless because the problem is linear. The maximum gradient represents the tracer front and is located slightly shoreward of the shelf break ($x = 100$ km). The gradient is clearly much stronger near the shelf break than even 10 km away on either side. Furthermore, the front is maintained largely unchanged for more than 500 km in the alongshelf direction, despite the fact that the velocity field has weakened considerably at that distance (Fig. 3).

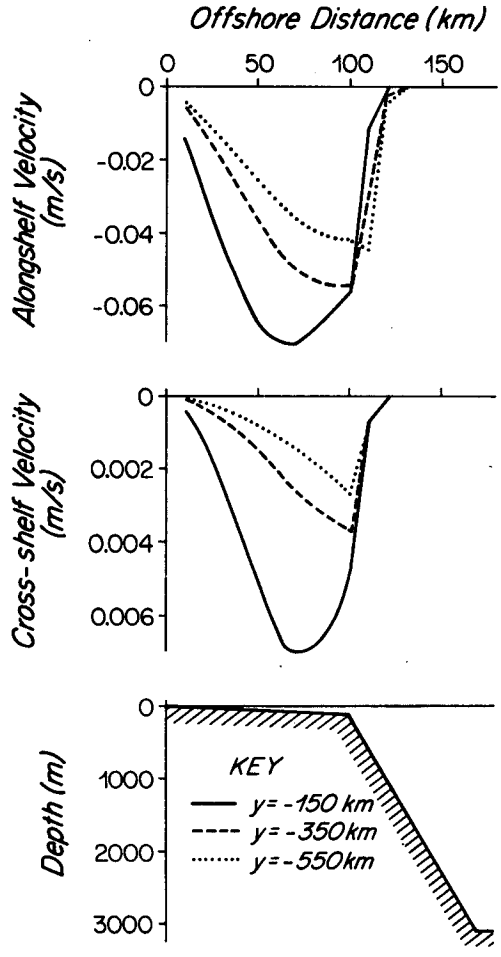

FIG. 3. Cross-shelf profiles of the alongshelf velocity (upper panel) and the cross-shelf velocity (middle panel) at several alongshelf locations. Bottom panel shows the model bottom topography.

4. Dynamics

The results of the previous section show that a tracer front may form near the shelf break in a barotropic coastal model. To understand the dynamics involved, it is helpful to study an extremely simple version of the problem. Suppose the ocean has a flat bottom ($h_x = 0$) and the velocity is constant and undirectional, $(u, v) = (0, -v_0)$. Equation (5) becomes

$$-v_0\epsilon_y = K(\epsilon_{xx} + \epsilon_{yy}). \quad (7)$$

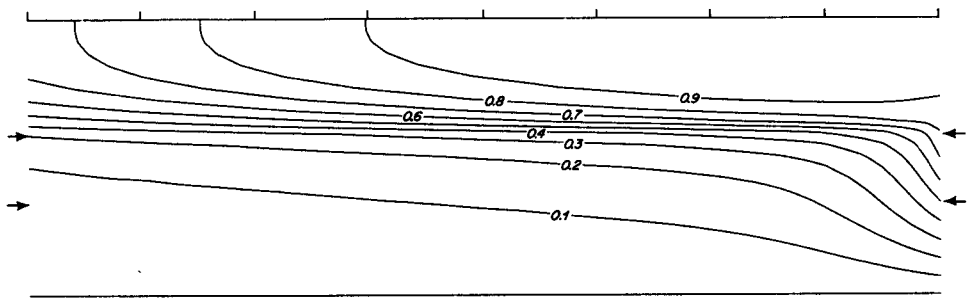

FIG. 4. Steady-state tracer distribution for the velocity field of Fig. 2 and the situation described in section 3. Contour interval is 0.1 (arbitrary units). Arrows denote the shelf break and the base of the continental slope.

With the boundary conditions stated in section 2 ($\epsilon_x = 0$ at $x = 0$, $\epsilon = 0$ at $x = L$) and the same upstream tracer distribution [$\epsilon_0 = \cos(\pi x/2L)$ at $y = 0$], the solution to (7) is

$$\epsilon = e^{\alpha_0 y} \cos(\pi x/2L) \tag{8}$$

where

$$\alpha_0 = \frac{-v_0}{2K}\left\{1 - \left[1 + 4\left(\frac{\pi}{2L}\right)^2\left(\frac{K}{v_0}\right)^2\right]^{1/2}\right\}.$$

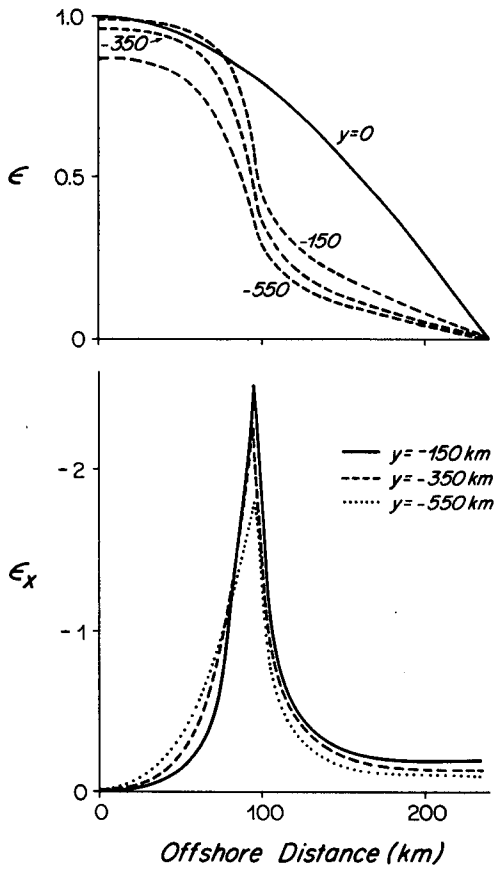

FIG. 5. Cross-shelf profiles of tracer concentration (upper panel) and of the cross-shelf gradient of tracer concentration (lower panel) at several alongshelf locations. Units are arbitrary.

The most obvious feature of (8) is that the solution has the same cross-shelf structure at each alongshelf location. Only the amplitude changes. Therefore, no front can form in this case, whereas the same upstream tracer distribution was transformed into a strong front within a short alongshelf distance using the model described in section 3. Next, consider the alongshelf decay scale (α_0^{-1}) of the initial tracer distribution. When diffusion dominates ($v_0 L/K \ll 1$), the alongshelf decay scale becomes $\alpha_0^{-1} \approx 2L/\pi = 153$ km. Thus, the initial distribution decays in a short alongshelf distance. When advection dominates ($v_0 L/K \gg 1$), the alongshelf decay scale becomes $\alpha_0^{-1} \approx (2L/\pi)^2(v_0/K) \gg 1$ which may be a very large distance. For the model of section 3, diffusion dominates in the deep ocean where velocities are very small, which leads to the rapid smoothing of the initial tracer distribution in the deep ocean (Fig. 4). In contrast, the shelf velocities are much larger and the initial tracer distribution is advected more rapidly downstream. For example, with $v_0 = -0.05$ m s^{-1}, the decay scale is $\alpha_0^{-1} \approx 12\,000$ km.

The difference in decay scales between the shelf and the deep ocean cannot alone account for the existence of the front. For example, consider introducing the same upstream tracer distribution in a flat-bottom ocean in which the upstream velocity shown in Fig. 2 is maintained unchanged throughout the model (i.e., $u = 0$ and v is independent of y). In this case, the tracer concentration becomes fairly homogeneous in the high velocity region. However, the diffusion in the low velocity region is now independent of x which leads to a linear decrease in tracer concentration (in x) toward the offshore wall. Thus, no front is formed. Similarly repeating the calculations described in section 3, but with a constant bottom slope everywhere [i.e., $h(x) = 10 + 0.001x$ for all x], does not lead to a front either.

The essential features of the dynamical model of section 3 which are necessary for the formation and maintenance of the front are 1) the velocity convergence near the shelf break and 2) the increase in bottom slope and depth seaward of the shelf break. These two features are intimately coupled (i.e., without the changing topography, the convergence vanishes), but

they play somewhat different roles in the frontal dynamics. This is revealed in Fig. 6 which shows the balance of terms from (5) as a function of cross-shelf distance at $y \doteq -350$ km. Over the shelf near the coast, the alongshelf advection ($v\epsilon_y$) balances the cross-shelf diffusion ($K\epsilon_{xx}$). As the shelf break is approached, the cross-shelf advection ($u\epsilon_x$) becomes important and eventually dominates over the alongshelf advection. Thus, just shoreward of the shelf break, diffusion gradually smooths the front by decreasing the tracer concentration while cross-shelf advection sharpens the front by moving tracer toward the shelf break. Slightly seaward of the front, cross-shelf diffusion gradually smooths the front by spreading tracer seaward (increasing the local tracer concentration) and reinforces the offshore advection. These two terms are then balanced by the effect of diffusion onto the steeper and deeper continental slope ($Kh_x\epsilon_x/h$). This apparent increase in diffusion (a statement of the fact that the depth-averaged tracer distribution must decrease when the tracer is spread over a deeper water depth) acts to decrease the tracer concentration near the shelf break, thus sharpening the front. As the depth increases, the velocities decrease, as does the bottom slope effect, leaving a purely diffusive balance in the deep ocean.

In summary, both along- and cross-shelf advection act to move tracer toward the shelf break. Seaward of the shelf break, the diffusion of tracer is substantially increased by the effect of the larger bottom slope and depth. The result is a strong tracer gradient near the shelf break, i.e., a tracer front. In the alongshelf direction, the velocity convergence near the shelf break maintains the front against both diffusion and the frictional decay of the advecting velocities.

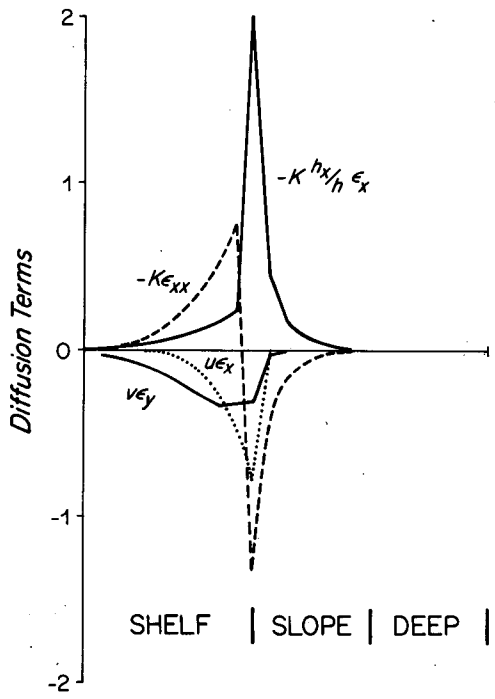

FIG. 6. Balance of terms in the advection–diffusion equation (5) across the shelf and slope at $y = -350$ km. Vertical lines denote shelf break and the base of the continental slope.

5. Discussion

The model presented here is intentionally oversimplified in order to illustrate the basic idea as simply as possible. However, many of the results seem to be fairly robust. For example, the eddy diffusivity used here is an order of magnitude larger than the value typically used in frontal models. If a smaller diffusivity is used in the present model, the front becomes sharper than shown in Figs. 4 and 5. Also, the form of bottom friction used here is not crucial. If r is assumed constant at some intermediate value, then the weaker shelf friction creates smaller seaward velocities over the shelf while the stronger friction in deep water leads to larger seaward velocities over the slope. The net result is a slightly weaker convergence near the shelf break and, hence, a slightly more diffuse front. Finally, the absence of upstream inflow in the deep ocean may also seem limiting. However, Chapman et al. (1986) have shown that the effect of upstream inflow in the deep region of a similar barotropic model is to create a stronger alongshelf flow near the shelf break and a more intense convergence there. Therefore, a deep upstream inflow would probably enhance the frontal formation and maintenance. In all of these cases, the qualitative results are unchanged.

The most serious shortcoming of the present model is clearly the assumption of vertical uniformity (i.e., no variations in the vertical) which has two important consequences: 1) the barotropic flow cannot cross isobaths easily, especially when moving off the shelf onto the much steeper continental slope, and 2) the tracer is vertically mixed throughout the water column everywhere (i.e., infinite vertical diffusion). Presumably, density stratification and finite vertical diffusion will alter the flow field and tracer distribution in the deep slope water (although the details are unknown). However, the flow field and tracer distribution near the shelf break, even in a more realistic situation, would probably be sufficiently uniform in the vertical so that the basic frontogenesis mechanism presented here would remain important. Indeed the point of the present model is merely to suggest a basic mechanism. An understanding of the effects of these and other simplifications (e.g., the neglect of horizontal momentum diffusion, the linearization of bottom friction, etc.) must await further modeling.

An interesting suggestion of the present results is that a shelf/slope front is more likely to be found along a shelf with a significant alongshelf mean flow and a distinct shelf break. For example, the Bering Sea shelf (Kinder and Schumacher, 1981) exhibits a shelf/slope

front which might be formed by a process similar to the one modeled here. Shelves with a less distinct shelf break, such as Peru (e.g., Brink et al., 1980), Oregon (e.g., Huyer et al., 1978), and northern California (e.g., Huyer, 1984), do not tend to exhibit shelf/slope fronts. There are, however, many other factors (e.g., wind forcing, buoyancy forcing, tidal mixing, etc.) which probably contribute to the formation of some shelf/slope fronts, so strong generalizations should not be made from the present results alone.

In conclusion the present results show that a steady barotropic coastal model (with no density variations) can form and maintain a tracer front near the shelf break. Whereas previous models have considered dynamically active density fronts, the present model offers an alternative mechanism for the formation and maintenance of the shelf/slope front in the Middle Atlantic Bight.

Acknowledgments. I thank R. C. Beardsley, R. W. Garvine and K. H. Brink for their encouragement and comments during the course of this work. Also, several helpful suggestions from anonymous reviewers were much appreciated. This research was supported by the National Science Foundation under Grant OCE84-17769.

REFERENCES

Beardsley, R. C., D. C. Chapman, K. H. Brink, S. R. Ramp and R. Schlitz, 1985: The Nantucket Shoals Flux Experiment (NSFE79). Part 1: A basic description of the current and temperature variability. *J. Phys. Oceanogr.*, **15,** 713–748.

Brink, K. H., D. Halpern and R. L. Smith, 1980: Circulation in the Peruvian upwelling system near 15°S. *J. Geophys. Res.*, **85,** 4036–4048.

Chapman, D. C., J. A. Barth, R. C. Beardsley and R. G. Fairbanks, 1986: On the continuity of mean flow between the Scotian Shelf and the Middle Atlantic Bight. *J. Phys. Oceanogr.*, **16,** 758–772.

Csanady, G. T., 1984: The influence of wind stress and river runoff on a shelf-sea front. *J. Phys. Oceanogr.*, **14,** 1383–1392.

Davis, R. E., 1985: Drifter observations of coastal surface currents during CODE: The statistical and dynamical views. *J. Geophys. Res.*, **90,** 4756–4772.

Fiadeiro, M. E., and G. Veronis, 1977: On weighted-mean schemes for the finite-difference approximation to the advection-diffusion equation. *Tellus,* **29,** 512–522.

Garrett, C., and E. Horne, 1978: Frontal circulation due to cabbeling and double diffusion. *J. Geophys. Res.*, **83,** 4651–4656.

Hsueh, Y., and B. Cushman-Roisin, 1983: On the formation of surface to bottom fronts over steep topography. *J. Geophys. Res.*, **88,** 743–750.

Huyer, A., 1984: Hydrographic observations along the CODE central line off northern California, 1981. *J. Phys. Oceanogr.*, **14,** 1647–1658.

——, R. L. Smith and E. J. C. Sobey, 1978: Seasonal differences in low-frequency current fluctuations over the Oregon continental shelf. *J. Geophys. Res.*, **83,** 5077–5089.

Kinder, T. H., and J. D. Schumacher, 1981: Hydrography over the continental shelf of the southeastern Bering Sea. *The Eastern Bering Sea Shelf: Oceanography and Resources,* Vol. 1, D. W. Hood and J. A. Calder, Eds., University of Washington Press, 31–52.

Lyne, V. D., and G. T. Csanady, 1984: A compilation and description of hydrographic transects of the Mid-Atlantic Bight shelf-break front. Woods Hole Oceanographic Institution Tech. Rep. WHOI-84-19, 290 pp.

Ou, H. W., 1983: Some two-layer models of the shelf-slope front: Geostrophic adjustment and its maintenance. *J. Phys. Oceanogr.*, **13,** 1798–1808.

Wang, D.-P., 1982: Effects of continental slope on the mean shelf circulation. *J. Phys. Oceanogr.*, **12,** 1524–1526.

——, 1984: Mutual intrusion of a gravity current and density front formation. *J. Phys. Oceanogr.*, **14,** 1191–1199.

Wright, W. R., 1983: Nantucket Shoals Flux Experiment Data Report I: Hydrography. NMFS, Northeast Fisheries Center, Woods Hole, MA; NOAA Tech. Memo. NMFS-F/NEC-23, 108 pp.